

Mirabegron, a $\beta 3$ -adrenoreceptor agonist, regulates right and left atrial arrhythmogenesis differently

CHAO-SHUN CHAN^{1,2}, FONG-JHIH LIN^{3,4}, CHIH-MIN LIU^{5,6}, YUNG-KUO LIN^{2,7}, YAO-CHANG CHEN⁴, CHUN-CHUN HSU^{8,9}, SATOSHI HIGA¹⁰, SHIH-ANN CHEN^{5,11,12} and YI-JEN CHEN^{7,13,14}

¹Department of Internal Medicine, Division of Cardiology, Taipei Medical University Hospital;

²Department of Internal Medicine, Division of Cardiology, School of Medicine;

³Graduate Institute of Medical Sciences, College of Medicine, Taipei Medical University, Taipei 11031;

⁴Department of Biomedical Engineering, National Defense Medical Center, Taipei 11490; ⁵Department of Medicine, Division of Cardiology, Heart Rhythm Center, Taipei Veterans General Hospital; ⁶Institute of Clinical Medicine and Faculty of Medicine, National Yang Ming Chiao Tung University, Taipei 11217; ⁷Department of Internal Medicine, Division of Cardiology, Wan-Fang Hospital, Taipei Medical University, Taipei 11696; ⁸School of Respiratory Therapy;

⁹Department of Internal Medicine, Division of Pulmonary Medicine, School of Medicine, College of Medicine, Taipei Medical University, Taipei 11031, Taiwan, R.O.C.; ¹⁰Cardiac Electrophysiology and

Pacing Laboratory, Division of Cardiovascular Medicine, Makiminato Central Hospital, Okinawa 9012131, Japan;

¹¹Cardiovascular Center, Taichung Veterans General Hospital, Taichung 40705; ¹²Department of Post-Baccalaureate Medicine, College of Medicine, National Chung Hsing University, Taichung 40227; ¹³Graduate Institute of Clinical Medicine, College of Medicine, Taipei Medical University, Taipei 11031; ¹⁴Cardiovascular Research Center, Wan-Fang Hospital, Taipei Medical University, Taipei 11696, Taiwan, R.O.C.

Received March 5, 2022; Accepted September 8, 2022

DOI: 10.3892/etm.2022.11656

Abstract. Mirabegron increases atrial fibrillation (AF) risk. The left atrium (LA) is the most critical 'substrate' for AF and has higher arrhythmogenesis compared with the right atrium (RA). The present study aimed to investigate the electrophysiological and arrhythmogenic effects of mirabegron on the LA and RA and clarify the potential underlying mechanisms. Conventional microelectrodes, a whole-cell patch clamp and a confocal microscope were used in rabbit LA and RA preparations or single LA and RA myocytes before and after mirabegron administration with or without cotreatment with KT5823 [a cyclic adenosine monophosphate (cAMP)-dependent protein kinase inhibitor]. The baseline action potential

duration at repolarization extents of 20 and 50% (but not 90%) were shorter in the LA than in the RA. Mirabegron at 0.1 and 1 μM (but not 0.01 μM) reduced the action potential duration at repolarization extents of 20 and 50% in the LA and RA. Mirabegron (0.1 μM) increased the occurrence of tachypacing-induced burst firing in the LA but not in the RA, where it was suppressed by KT5823 (1 μM). Mirabegron (0.1 μM) increased the L-type Ca^{2+} current ($I_{\text{Ca-L}}$), ultrarapid component of delayed rectifier K^{+} current (I_{Kur}), Ca^{2+} transients and sarcoplasmic reticulum Ca^{2+} content but reduced transient outward K^{+} current (I_{to}) in the LA myocytes. However, mirabegron did not change the Na^{+} current and delayed rectifier K^{+} current in the LA myocytes. Moreover, pretreatment with KT5823 (1 μM) inhibited the effects of mirabegron on $I_{\text{Ca-L}}$, I_{to} and I_{Kur} in the LA myocytes. Furthermore, in the RA myocytes, mirabegron reduced $I_{\text{Ca-L}}$ but did not change I_{to} . In conclusion, mirabegron differentially regulates electrophysiological characteristics in the LA and RA. Through the activation of the cAMP-dependent protein kinase pathway and induction of Ca^{2+} dysregulation, mirabegron may increase LA arrhythmogenesis, leading to increased AF risk.

Introduction

$\beta 3$ -Adrenoreceptors ($\beta 3\text{ARs}$) are involved in adipocyte metabolism, gut relaxation and vascular vasodilation (1). Mirabegron is a selective $\beta 3\text{AR}$ agonist approved for overactive bladder treatment (2-4). Although the role of $\beta 3\text{AR}$ in adipose, intestinal and vascular tissues is well established, its

Correspondence to: Dr Yi-Jen Chen, Graduate Institute of Clinical Medicine, College of Medicine, Taipei Medical University, 250 Wu-Hsing, Taipei 11031, Taiwan, R.O.C.
E-mail: yjchen@tmu.edu.tw

Dr Chun-Chun Hsu, Department of Internal Medicine, Division of Pulmonary Medicine, School of Medicine, College of Medicine, Taipei Medical University, 250 Wu-Hsing Street, Taipei 11031, Taiwan, R.O.C.
E-mail: chunhsu@tmu.edu.tw

Key words: mirabegron, $\beta 3$ -Adrenoreceptors, atrial fibrillation, left atrium, right atrium

existence and function in the heart remain unclear. In human cardiomyocytes, β 3ARs couple with the inhibitory G protein to exhibit a negative inotropic effect, which counterbalances the effects of β 1- and β 2-adrenergic stimulation in heart failure by increasing nitric oxide production (5,6). However, the differential expression of β 3ARs can lead to distinct effects in tissues and cells. β 3ARs can stimulate the L-type Ca^{2+} current ($I_{\text{Ca-L}}$) in human atrial cells and enhance atrial tissue contractility through the cyclic adenosine monophosphate (cAMP)-dependent protein kinase pathway (7).

In clinical trials, the most commonly reported cardiovascular adverse events in patients receiving mirabegron for overactive bladder are hypertension, tachycardia and atrial fibrillation (AF) (8-10). The number of older patients with AF risk receiving mirabegron treatment has increased recently. However, the mechanisms underlying the potential arrhythmogenic effects of mirabegron remain unclear. Mirabegron might change cardiac electrophysiological characteristics due to its effects on $I_{\text{Ca-L}}$ activation through the cAMP-dependent pathway, possibly resulting in Ca^{2+} dysregulation (11-15). The left atrium (LA), the most critical 'substrate' of AF (16,17), is vulnerable to oxidative stress and has higher arrhythmogenesis compared with the right atrium (RA) (18). Moreover, our previous studies indicate that the LA is more susceptible to hydrogen sulfide- and chronic obstructive pulmonary disease-related atrial arrhythmogenesis than is the RA (19,20). The differential arrhythmogenic effects between the LA and RA facilitate the maintenance of atrial arrhythmogenesis. Since mirabegron alters cardiac electrophysiological characteristics, resulting in arrhythmogenesis, the effects of mirabegron may differ between the LA and RA. Mirabegron may induce atrial arrhythmogenesis through differential arrhythmogenic effects between the LA and RA. Therefore, the present study aimed to investigate the differences in the effects of mirabegron on the electrophysiological activities of the LA and RA and clarify the underlying mechanisms.

Materials and methods

Rabbit atrial tissue preparations. All the experimental procedures were approved by the Institutional Animal Care and Use Committee of Taipei Veterans General Hospital, Taipei, Taiwan (approval no. IACUC-2021-011). Furthermore, the experimental protocols conformed to the institutional guideline for the care and use of laboratory animals as well as the Guide for the Care and Use of Laboratory Animals, published by the US National Institutes of Health (21). Male New Zealand white rabbits ($n=36$; weight, 2.5-3.5 kg; age, 6-8 months) used in the present study were purchased from Animal Health Research Institute (Council of Agriculture, Executive Yuan). All of the rabbits were housed in a temperature- and humidity-controlled environment (20-22°C; 50-70% humidity) with a 12 h light/dark cycle, raised in stainless steel cages and had free access to food and water. Rabbits were anesthetized with an intramuscular injection of a mixture of zoletil (10 mg/kg; Virbac) and xylazine (5 mg/kg; Bayer AG) and sacrificed with an overdose of inhaled isoflurane (5% in oxygen; Panion & BF Biotech, Inc.) from a precision vaporizer (22,23). The anesthesia dosage was confirmed to be adequate on the basis of the absence of corneal reflexes and motor responses to pain stimuli. The hearts were

excised through midline thoracotomy. The tissue preparations ($1 \times 1.5 \text{ cm}^2$) of the LA and RA were separated from the LA and RA appendages, respectively. Electropharmacological measurements were obtained within 2 h after the separation. Tissue preparations (1-1.5 cm) of the RA and LA were superfused at 37°C with normal Tyrode's solution composed of NaCl (137 mM), KCl (4 mM), NaHCO_3 (15 mM), NaH_2PO_4 (0.5 mM), MgCl_2 (0.5 mM), CaCl_2 (2.7 mM) and dextrose (11 mM) at a constant rate of 3 ml/min. Tyrode's solution was saturated with a mixture of 97% O_2 and 3% CO_2 and its pH was adjusted to 7.4 with NaOH.

Electropharmacological experiments. The transmembrane action potentials of the RA and LA were recorded using machine-pulled glass capillary microelectrodes filled with KCl (3 M) (20). The microelectrodes were connected to an FD223 electrometer (World Precision Instruments) under 150-mg tension. The electrical events were simultaneously displayed on a Gould 4072 oscilloscope (Gould) and a Gould TA11 recorder (Gould). Electrical stimuli were applied using a Grass S88 stimulator (Grass Instruments) through a Grass SIU5B stimulus isolation unit. The action potential parameters were measured by applying 2-Hz electrical stimuli. The action potential amplitude (APA) was calculated as the difference between the resting membrane potential (RMP) and the peak of action potential depolarization. The action potential duration (APD) at repolarization extents of 90, 50 and 20% of the APD were measured and designated as APD_{90} , APD_{50} and APD_{20} , respectively. Burst firing was defined as the occurrence of accelerated spontaneous activities (faster than the basal rate) with sudden onset and termination. The same RA and LA tissue preparations were sequentially treated with different concentrations (0.01, 0.1 and 1 μM) of mirabegron (Avara Pharmaceutical Technologies) in Tyrode's solution for 30 min to investigate the electrophysiological effects of mirabegron with and without 1 μM KT5823 (an inhibitor of cAMP-dependent protein kinase; MilliporeSigma).

Ionic current measurements. Single LA and RA myocytes from rabbits were enzymatically dissociated, as described previously (24). Whole-cell patch clamp recordings of the single LA and RA myocytes were obtained before and after the administration of mirabegron (0.1 μM) with or without KT5823 (1 μM) using an Axopatch 1D amplifier (Axon Instruments) at $35 \pm 1^\circ\text{C}$. The ionic currents were recorded at ~3-5 min after rupture or perforation to obtain measurements before ion channel activity decay over time. A small hyperpolarizing step from a holding potential of -50 mV to a test potential of -55 mV for 80 msec was delivered at the beginning of each experiment. The area under the capacitive current curve was divided using the applied voltage step to obtain the total cell capacitance. In general, 60-80% series resistance was electronically compensated. Ionic currents were recorded in the current- and voltage-clamp modes.

The Na^+ current (I_{Na}) was measured during depolarization from a holding potential of -120 mV to testing potentials ranging from -80-0 mV in 10-mV increments for 40 msec at a 3-Hz frequency and at room temperature ($25 \pm 1^\circ\text{C}$). The external solution contained NaCl (5 mM), CsCl (133 mM), MgCl_2 (2 mM), CaCl_2 (1.8 mM), nifedipine (0.002 mM),

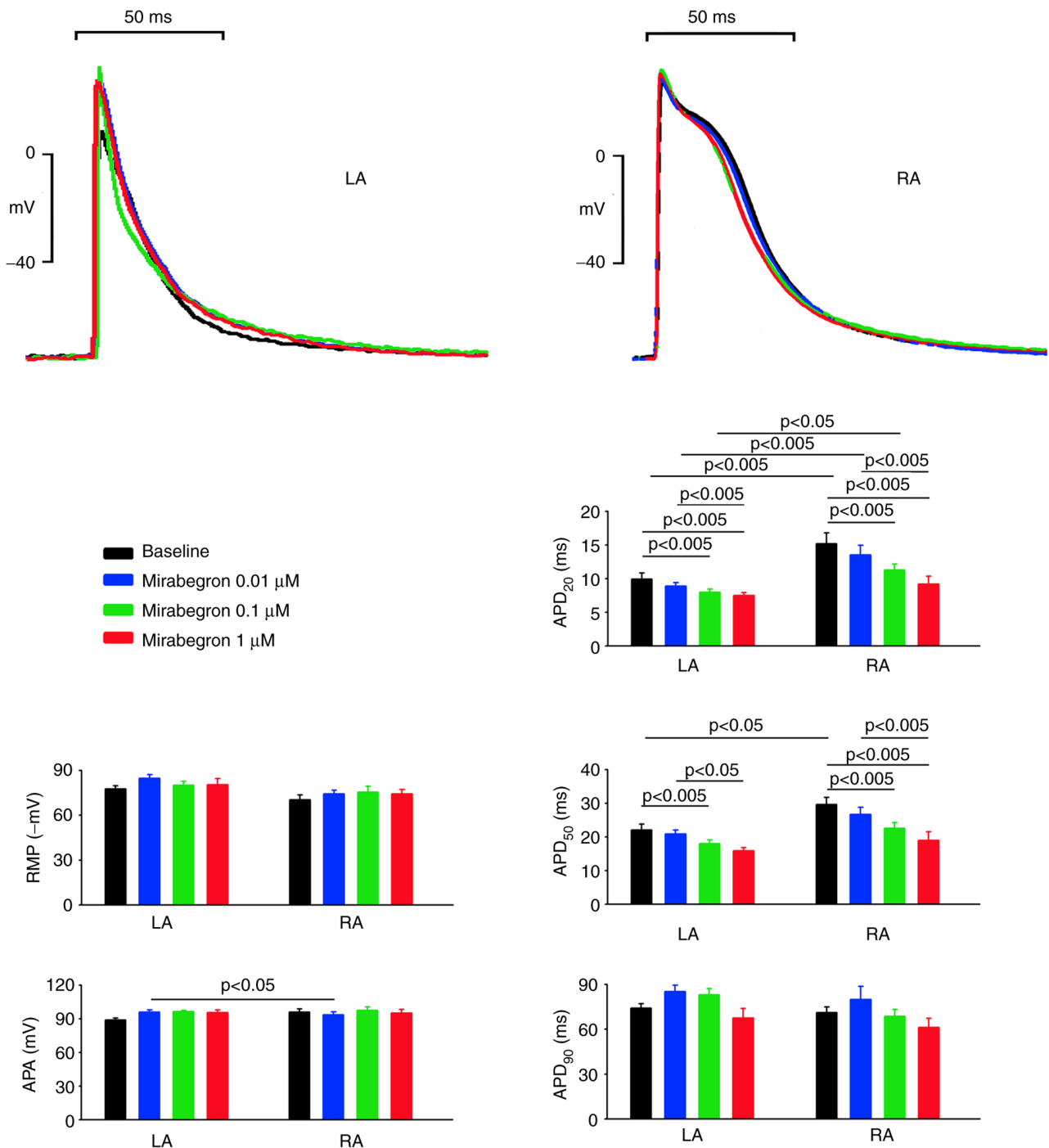


Figure 1. Effects of mirabegron on atrial electrical activity. Tracings of action potentials (upper panel) and average data (lower panel) of action potential parameters in the LA (n=10) and RA (n=10) before and after mirabegron treatment. LA, left atrium; RA, right atrium; APA, action potential amplitude; RMP, resting membrane potential; APD₂₀, action potential duration (APD) at repolarization extent of 20% of the APD; APD₅₀, APD at repolarization extent of 50% of the APD; APD₉₀, APD at repolarization extent of 90% of the APD.

4-(2-hydroxyethyl)-1-piperazineethanesulfonic acid (HEPES; 5 mM) and glucose (5 mM) adjusted to a pH of 7.3 with KOH. The micropipettes were filled with a solution containing CsCl (133 mM), NaCl (5 mM), ethylene glycol-bis (β-aminoethyl ether)-N,N,N',N'-tetraacetic acid (EGTA; 10 mM), tetraethylammonium chloride (TEACl; 20 mM), MgATP (5 mM) and HEPES (5 mM) titrated to a pH of 7.3 with CsOH.

I_{Ca-L} was measured as an inward current during depolarization from a holding potential of -50 mV to test potentials ranging from -40 to +60 mV in 10-mV increments for 300 msec

at a 0.1-Hz frequency by using a perforated patch clamp with amphotericin B. The external solution contained TEACl (20 mM), CsCl (133 mM), HEPES (10 mM), MgCl₂ (0.5 mM), CaCl₂ (1.8 mM) and glucose (10 mM) titrated to a pH of 7.4 with NaOH. Tetrodotoxin (10 μM) and 4-aminopyridine (2 mM) were added to the external solution to block Na⁺ channels and transient outward K⁺ current (I_{to}), respectively. The micropipettes were filled with a solution containing CsCl (130 mM), MgCl₂ (1 mM), Mg₂ATP (5 mM), HEPES (10 mM), EGTA (10 mM), NaGTP (0.1 mM) and Na₂ phosphocreatine

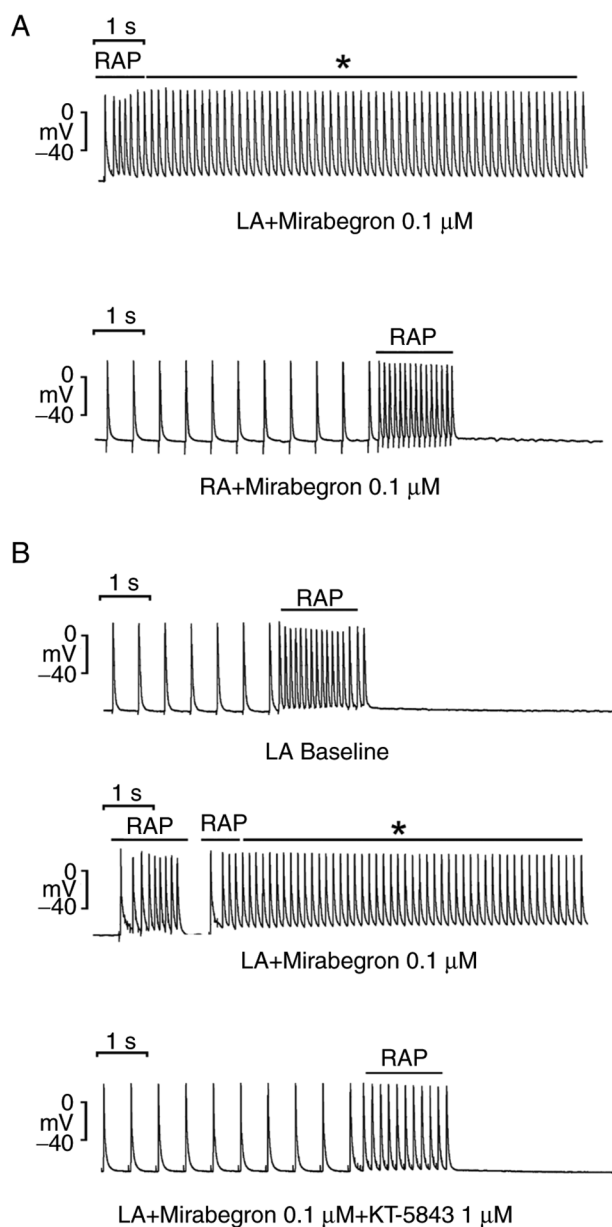


Figure 2. Effects of mirabegron on atrial arrhythmogenesis. (A) Tracings indicating that burst firing was induced by 20-Hz tachypacing and 0.1 μ M mirabegron treatment in the LA but not in the RA. (B) Tracings indicating the effects of 1 μ M KT5823 on burst firing induced by 20-Hz tachypacing and 0.1 μ M mirabegron treatment in the LA. *Denotes burst firing induced by 20-Hz tachypacing and mirabegron infusion. LA, left atrium; RA, right atrium; RAP, rapid atrial pacing.

(5 mM) titrated to a pH of 7.2 with CsOH. Steady-state inactivation of I_{Ca-L} was evaluated using a standard protocol consisting of a 300-msec prepulse and a 150-msec test pulse. The peak current elicited by the test pulse was divided by the maximal current and plotted as a function of prepulse voltage. Data points were fitted using a Boltzmann function. Recovery from I_{Ca-L} inactivation was assessed using a two-pulse protocol with a 200-msec prepulse and test pulse (from -80 to $+10$ mV) separated using varying time intervals. Data points were fitted with a single-exponential function (25).

I_{Na} was estimated using a double-pulse protocol. A 30-msec prepulse from -80 to -40 mV was used to inactivate the Na^+ channels and this was followed by a 300-msec test pulse increasing

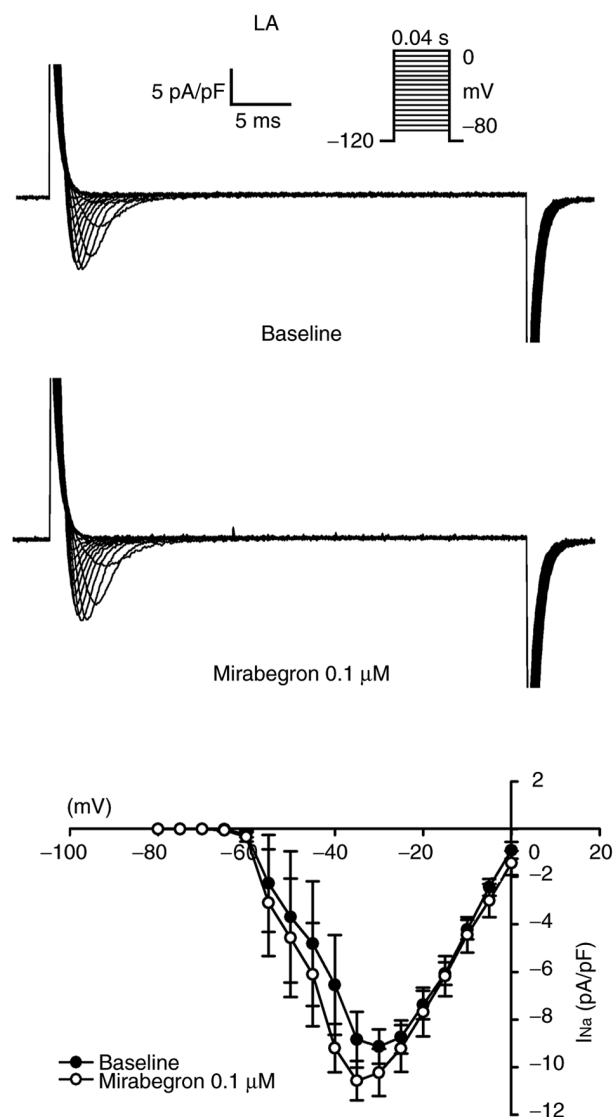


Figure 3. Effects of mirabegron on I_{Na} in LA myocytes. Tracings and current-voltage relationship of I_{Na} in the LA myocytes ($n=11$) before and after 0.1 μ M mirabegron treatment. Insets in the current traces show various clamp protocols. I_{Na} , Na^+ current; LA, left atrium.

to $+60$ mV in 10-mV increments at a 0.1-Hz frequency. $CdCl_2$ (200 μ M) was added to the bath solution for I_{Ca-L} inhibition. I_{Na} was calculated as the difference between the peak outward current and steady-state current. The external solution contained NaCl (137 mM), KCl (5.4 mM), HEPES (10 mM), $MgCl_2$ (0.5 mM), $CaCl_2$ (1.8 mM) and glucose (10 mM) titrated to a pH of 7.4 with NaOH. The micropipettes were filled with a solution containing KCl (20 mM), K-aspartate (110 mM), $MgCl_2$ (1 mM), $MgATP$ (5 mM), HEPES (10 mM), EGTA (0.5 mM), NaGTP (0.1 mM) and Na_2 phosphocreatine (5 mM) titrated to a pH of 7.2 with KOH.

The ultrarapid component of the delayed rectifier K^+ current (I_{Kur}) was examined using a double-pulse protocol, consisting of a 100-msec depolarizing prepulse increasing to $+40$ mV from a holding potential of -50 mV, which was followed by 150-msec voltage steps from -40 to $+60$ mV in 10-mV increments at room temperature to provide an adequate temporal resolution. I_{Kur} was measured as the 4-aminopyridine (1 mM)-sensitive current. The external solution contained

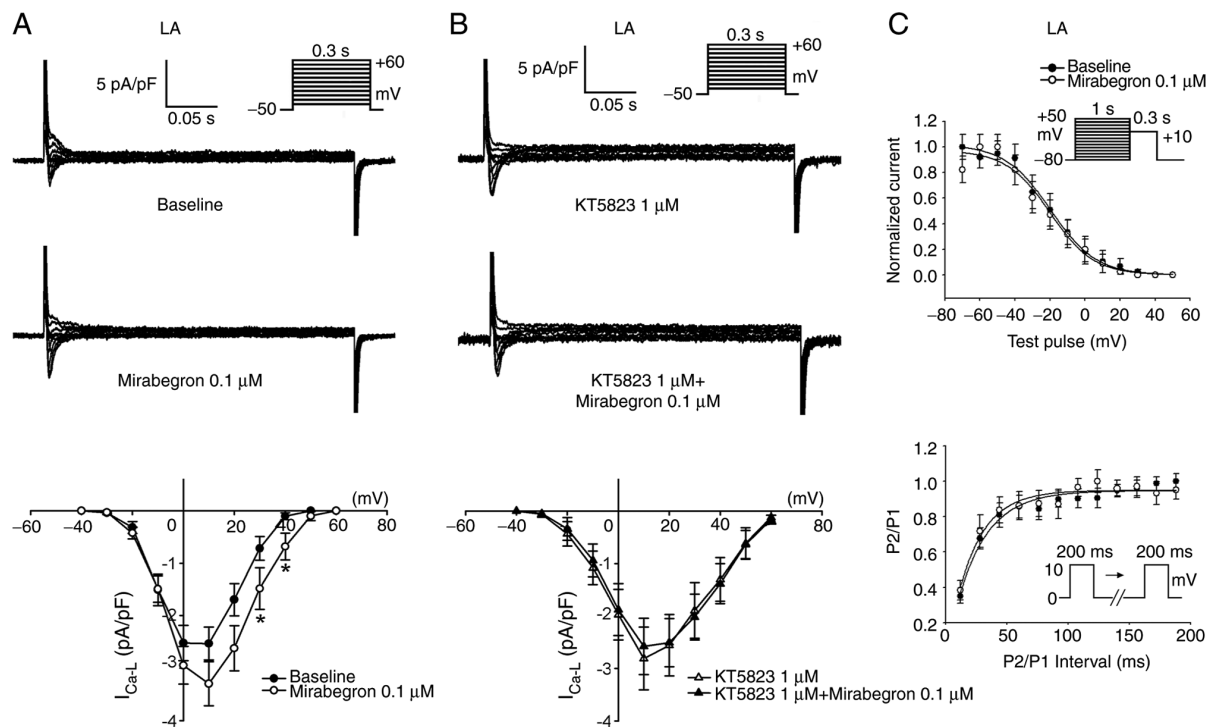


Figure 4. Effects of mirabegron on I_{Ca-L} in LA myocytes. (A) Tracings and current-voltage relationship of I_{Ca-L} in the LA myocytes (n=11) before and after 0.1 μ M mirabegron treatment. (B) Inhibition of these effects (n=10) with 1 μ M KT5823 pretreatment. (C) Voltage-dependent inactivation (upper panel) and recovery kinetics (lower panel) of I_{Ca-L} in the LA myocytes (n=11) before and after 0.1 μ M mirabegron treatment. Insets in the current traces show various clamp protocols. *P<0.05 vs. baseline. I_{Ca-L} , Ca^{2+} current; LA, left atrium.

NaCl (137 mM), KCl (5.4 mM), HEPES (10 mM), $MgCl_2$ (0.5 mM), $CaCl_2$ (1.8 mM) and glucose (10 mM) titrated to a pH of 7.4 with NaOH. The micropipettes were filled with a solution containing KCl (20 mM), K-aspartate (110 mM), $MgCl_2$ (1 mM), MgATP (5 mM), HEPES (10 mM), EGTA (0.5 mM), NaGTP (0.1 mM) and Na_2 phosphocreatine (5 mM) titrated to a pH of 7.2 with KOH.

The delayed rectifier K^+ current ($I_{Kr-tail}$) was measured as the outward peak tail current density after 3 sec of prepulse increasing from a holding potential of -40 mV to a voltage between -40 and +60 mV in 10-mV steps at a 0.1-Hz frequency in the presence of chromanol 293B (30 μ M) and $CdCl_2$ (200 μ M) in normal Tyrode's solution. The micropipettes were filled with a solution containing KCl (120 mM), $MgCl_2$ (5 mM), $CaCl_2$ (0.36 mM), EGTA (5 mM), HEPES (5 mM), glucose (5 mM), K_2ATP (5 mM), Na_2CrP (5 mM) and NaGTP (0.25 mM) adjusted to a pH of 7.2 with KOH.

Measurements of Ca^{2+} transients (Ca^{2+i}) and intracellular Ca^{2+} . Intracellular Ca^{2+} was measured in single LA myocytes, as described previously (26). In brief, LA myocytes were loaded with fluorescent Ca^{2+} (10 μ M) fluo-3/AM for 30 min at room temperature. After intracellular hydrolysis of fluo-3/AM for 30 min, the excess extracellular dye was removed by changing the bath solution. Fluo-3 fluorescence was triggered using a 488-nm argon-ion laser line, with the emission recorded at >515 nm. The LA myocytes were repetitively scanned at 2-msec intervals for line scan imaging (8-bit). Fluorescence imaging was performed using a laser scanning confocal microscope (Zeiss LSM 510; Zeiss GmbH) and an inverted microscope (Axiovert 100; Zeiss GmbH). To exclude

variations in the fluorescence intensity due to different volumes of injected dye and to correct for variations in dye concentrations, the fluorescent signals were calculated by normalizing the fluorescence (F) against the baseline fluorescence (F_0); in this manner, reliable information was obtained on transient intracellular Ca^{2+} changes from baseline values [$\Delta F = (F - F_0)/F_0$]. The intracellular Ca^{2+} changes, including transient Ca^{2+i} , peak systolic Ca^{2+i} and diastolic Ca^{2+i} , were obtained during a 2-Hz field stimulation with 10-msec twice-threshold-strength square-wave pulses. Through the addition of 20 mM caffeine after electric stimulation at 2 Hz for at least 30 sec, the estimated sarcoplasmic reticulum (SR) Ca^{2+} content was measured as the total SR Ca^{2+} content from the peak amplitude of the caffeine induced Ca^{2+i} .

Statistical analysis. All continuous variables are expressed as means \pm standard deviations. Paired t test, one-way or two-way repeated-measures analysis of variance with the Bonferroni post hoc test was used to compare the difference between LA and RA or the effects of mirabegron on the LA and RA tissue preparations and isolated single myocytes. The McNemar test was used to compare the incidence of burst firing before and after drug administration in the LA and RA tissue preparations. P<0.05 was considered to indicate a statistically significant difference.

Results

Effects of mirabegron on atrial electric activity. As shown in Fig. 1, the baseline APA and RMP of the LA and RA were similar. However, the baseline APD_{20} and APD_{50} but not

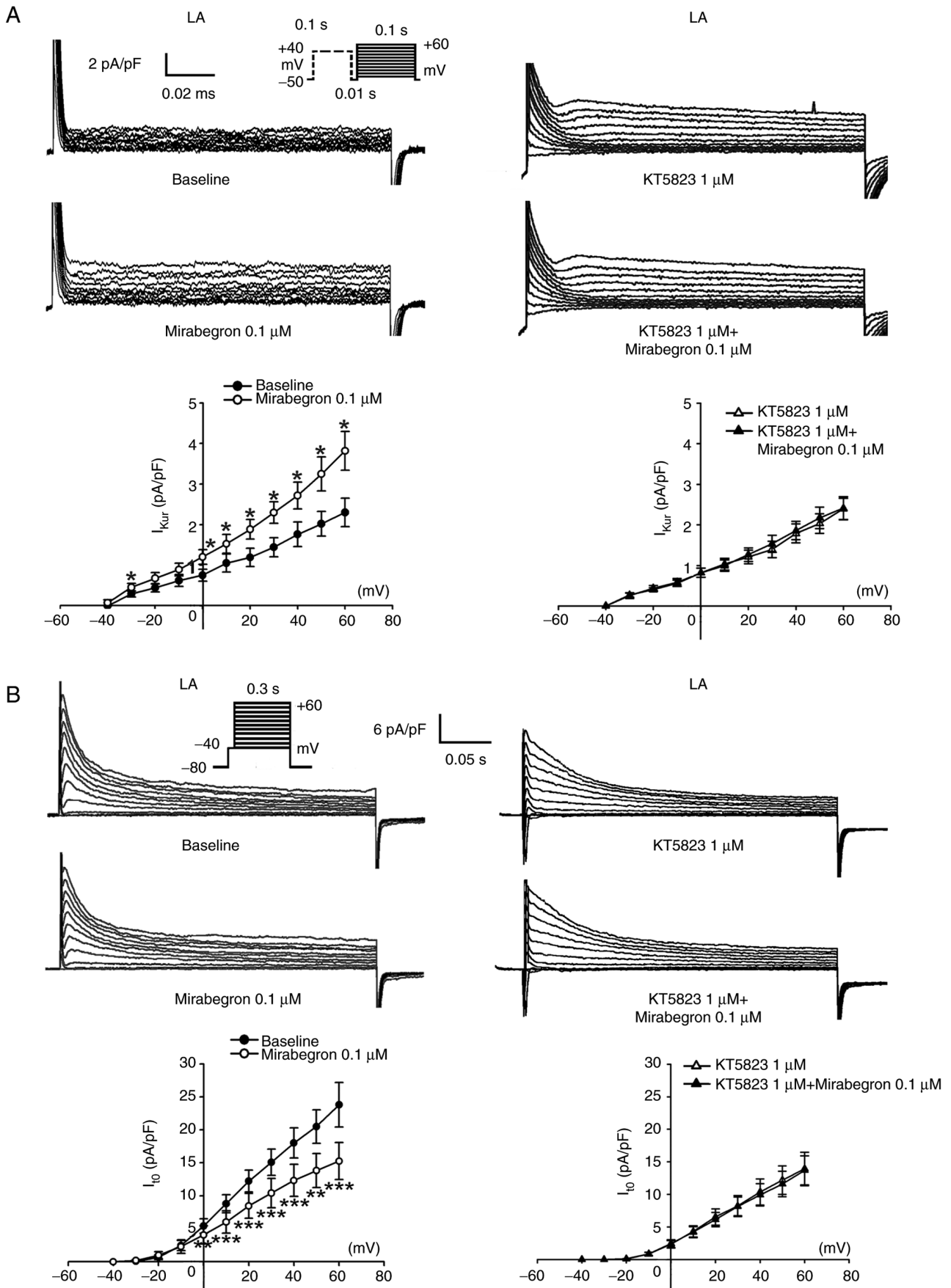


Figure 5. Effects of mirabegron on $I_{K_{ur}}$ and I_{to} in LA myocytes. (A) Tracings and current-voltage relationship of $I_{K_{ur}}$ in the LA myocytes ($n=10$) before and after 0.1 μ M mirabegron treatment (left panel) and inhibition of these effects ($n=11$) with 1 μ M KT5823 pretreatment (right panel). (B) Tracings and current-voltage relationship of I_{to} in the LA myocytes ($n=9$) before and after 0.1 μ M mirabegron treatment (left panel) and inhibition of these effects ($n=9$) with 1 μ M KT5823 pretreatment (right panel). Insets in the current traces show various clamp protocols. * $P<0.05$, ** $P<0.01$ and *** $P<0.005$ vs. baseline. $I_{K_{ur}}$, ultrarapid component of delayed rectifier K^+ current; I_{to} , transient outward K^+ current; LA, left atrium.

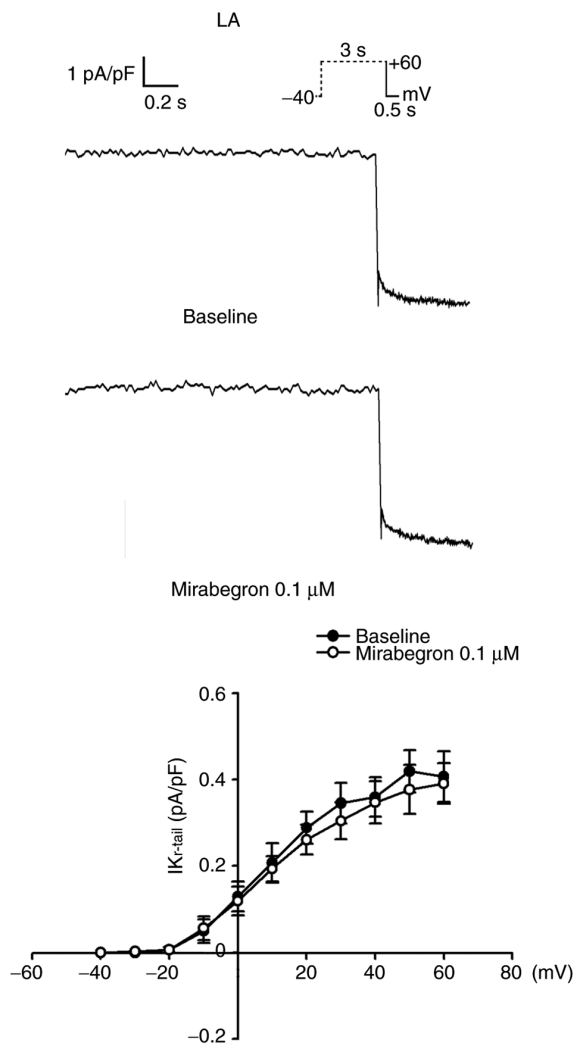


Figure 6. Effects of mirabegron on $I_{K_{r-tail}}$ in LA myocytes. Tracings and current-voltage relationship of $I_{K_{r-tail}}$ in the LA myocytes (n=10) before and after 0.1 μ M mirabegron treatment. Insets in the current traces show various clamp protocols. $I_{K_{r-tail}}$, delayed rectifier K^+ current; LA, left atrium.

APD₉₀ were shorter in the LA than in the RA. Mirabegron, at 0.1 and 1 μ M (but not 0.01 μ M), reduced the APD₂₀ and APD₅₀ of the LA, but it did not alter the APA, RMP, or APD₉₀ of the LA at 0.01, 0.1, or 1 μ M. Similarly, mirabegron at 0.1 and 1 μ M (but not 0.01 μ M), reduced the APD₂₀ and APD₅₀ of the RA, but it did not alter the APA, RMP, or APD₉₀ of the RA at 0.01, 0.1, or 1 μ M. Moreover, as shown in Fig. 2A, under mirabegron treatment at 0.1 and 1 μ M (but not 0.01 μ M), 20-Hz tachypacing induced burst firing in 7 of the 10 LAs (70% vs. 0% at baseline, $P<0.05$). By contrast, 20-Hz tachypacing did not induce burst firing in any of the 10 RAs under mirabegron treatment at 0.01, 0.1 and 1 μ M. However, with the addition of KT5823 (1 μ M), burst firing was suppressed in 5 of the 6 LAs (83.3% vs. 0% at baseline, $P<0.05$, Fig. 2B).

Effects of mirabegron on ionic currents and Ca^{2+} homeostasis. The present study compared baseline I_{Ca-L} and I_{to} in the LA and RA myocytes and found that the LA myocytes had a smaller I_{Ca-L} but a larger I_{to} than the RA myocytes (Fig. S1).

The effects of mirabegron on I_{Na} , I_{Ca-L} , I_{to} , I_{Kur} and $I_{K_{r-tail}}$ in the LA myocytes were investigated. As shown in Fig. 3, I_{Na}

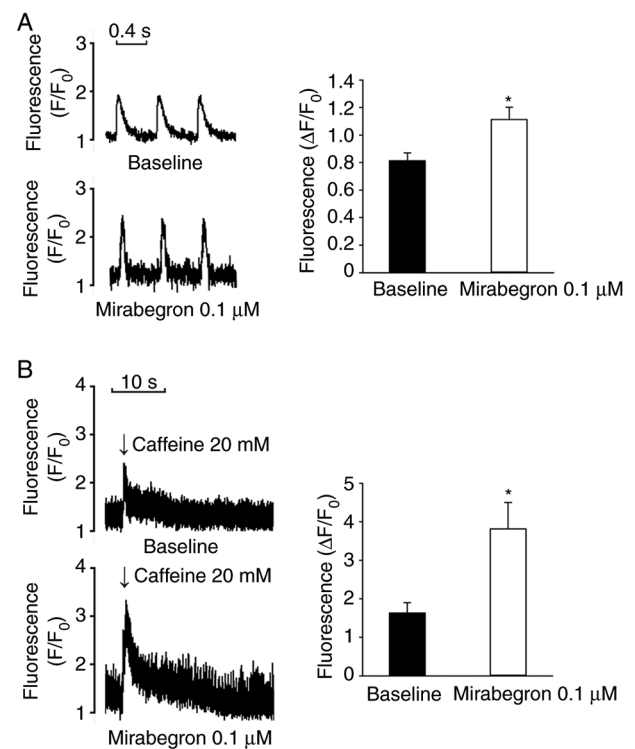


Figure 7. Effects of mirabegron on $Ca^{2+}i$ and SR Ca^{2+} content in LA myocytes. (A) Tracings (left panel) and average data (right panel) of $Ca^{2+}i$ before (n=11) and after (n=15) 0.1 μ M mirabegron treatment in the LA myocytes. (B) Tracings (left panel) and average data (right panel) of SR Ca^{2+} content before (n=9) and after (n=12) 0.1 μ M mirabegron treatment in the LA myocytes. * $P<0.05$ vs. baseline. $Ca^{2+}i$, Ca^{2+} transients; SR, sarcoplasmic reticulum; LA, left atrium.

in the LA myocytes remained unchanged after mirabegron (0.1 μ M) treatment. Moreover, mirabegron (0.1 μ M) significantly increased I_{Ca-L} in the LA myocytes (Fig. 4A). KT5823 (1 μ M) pretreatment attenuated the effects of mirabegron on I_{Ca-L} (Fig. 4B). Additionally, as shown in Fig. 4C, mirabegron (0.1 μ M) did not alter the voltage-dependent inactivation of I_{Ca-L} (-32.4 ± 5.3 mV vs. -29.5 ± 4.2 mV, $P>0.05$) and time constants of recovery from inactivation of I_{Ca-L} (40.5 ± 21.4 msec vs. 53.1 ± 13.4 msec, $P>0.05$).

As shown in Fig. 5, mirabegron (0.1 μ M) significantly increased I_{Kur} but reduced I_{to} . Similarly, KT5823 (1 μ M) pretreatment attenuated the effects of mirabegron on I_{Kur} and I_{to} . By contrast, $I_{K_{r-tail}}$ in the LA myocytes remained unchanged after 0.1 μ M mirabegron treatment (Fig. 6). Moreover, mirabegron (0.1 μ M) increased $Ca^{2+}i$ and SR Ca^{2+} contents in the LA myocytes (Fig. 7).

To clarify whether mirabegron may have different ionic effects between RA and LA myocytes, the present study investigated the effects of mirabegron on I_{Ca-L} and I_{to} in the RA myocytes. In contrast to the effects of mirabegron on I_{Ca-L} and I_{to} in LA myocytes, mirabegron (0.1 μ M) reduced I_{Ca-L} and did not alter I_{to} in RA myocytes (Fig. 8).

Discussion

The present study, for the first time to the best of the authors' knowledge, found that mirabegron significantly increased the inducibility of burst firing through tachypacing in the LA but

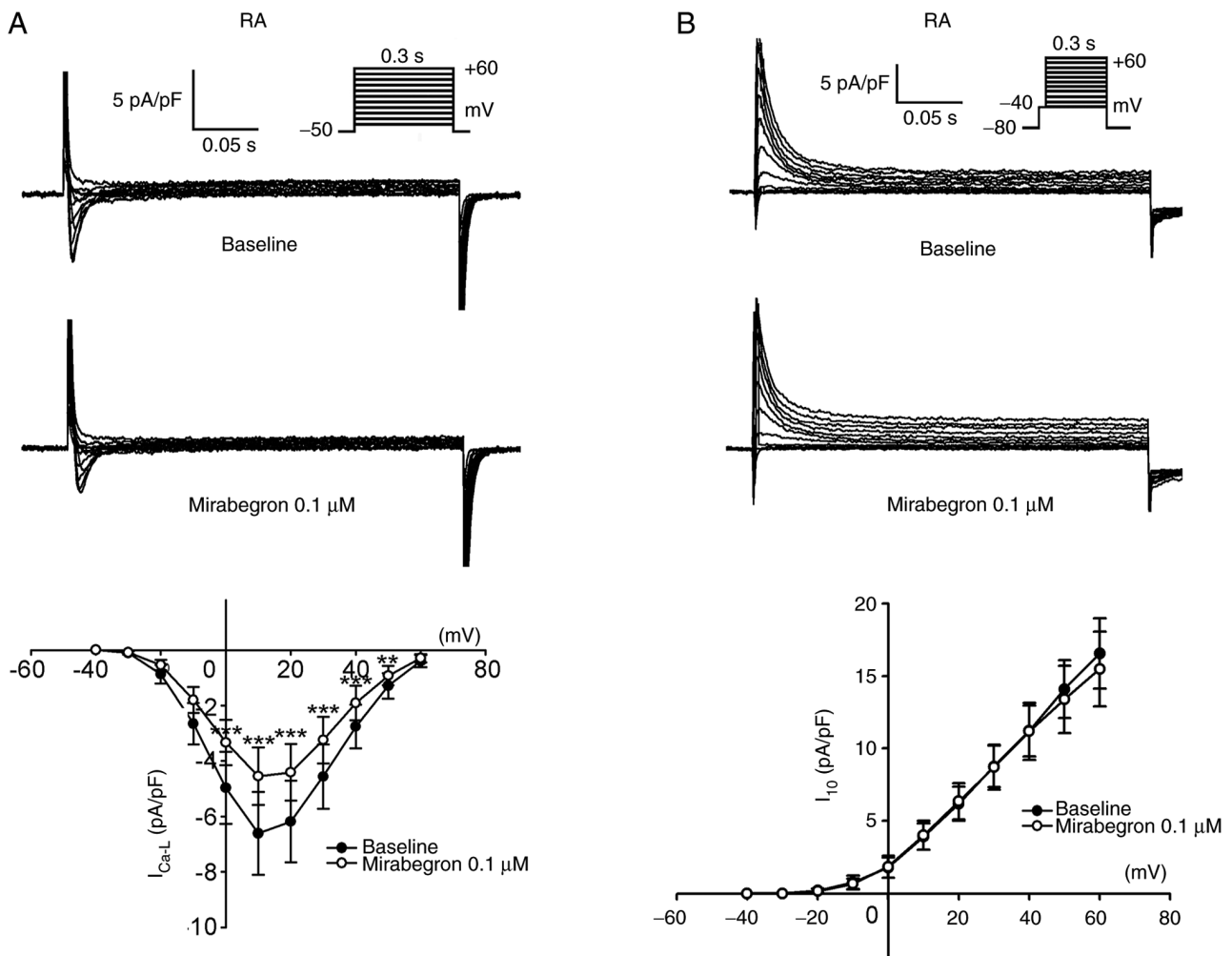


Figure 8. Effects of mirabegron on I_{Ca-L} and I_{to} in RA myocytes. Tracings and current-voltage relationship of (A) I_{Ca-L} (n=12) and (B) I_{to} (n=10) in the RA myocytes before and after 0.1 μ M mirabegron treatment. Insets in the current traces show various clamp protocols. ** $P < 0.01$ and *** $P < 0.005$ vs. baseline. I_{Ca-L} , Ca^{2+} current; I_{to} , transient outward K^+ current; RA, right atrium.

not in the RA, suggesting that mirabegron differentially induces atrial arrhythmogenesis in the LA but not the RA. Moreover, the results indicated that KT5823, a cAMP-dependent protein kinase inhibitor, suppressed burst firing induced by 20-Hz tachypacing and mirabegron in the LA. These results suggested that the cAMP-dependent protein kinase pathway may serve a role in mirabegron-induced atrial arrhythmogenesis.

cAMP-dependent protein kinase phosphorylates several key intracellular Ca^{2+} regulatory proteins such as Ca^{2+} channels, sarco/endoplasmic reticulum Ca^{2+} -ATPase (SERCA), phospholamban (PLB), ryanodine receptor channel (RyR) and Na^+/Ca^{2+} exchangers (NCXs). In particular, cAMP-dependent protein kinase activation increases PLB, RyR and NCX phosphorylation, resulting in Ca^{2+} dysregulation and arrhythmogenesis (11-13,27). In the whole-cell patch clamp experiments, mirabegron significantly increased I_{Ca-L} in the LA myocytes. A prolonged increase in I_{Ca-L} causes Ca^{2+} overload, which may contribute to arrhythmogenesis (28). Moreover, KT5823 pretreatment inhibited the effects of mirabegron on I_{Ca-L} in the LA myocytes in the current study and mirabegron significantly increased Ca^{2+}_i and SR Ca^{2+} content in these myocytes. Therefore, the findings indicated that mirabegron may change the electrophysiological characteristics of the LA and cause LA

arrhythmogenesis by activating the cAMP-dependent protein kinase pathway and inducing Ca^{2+} dysregulation.

In the present study, mirabegron was found to accelerate LA and RA repolarization, which possibly reduces the effective refractory period, favoring the genesis of reentry (29). The results of the present study revealed that mirabegron significantly shortened the APD_{20} and APD_{50} but not APD_{90} of the LA and RA. In theory, APD_{20} and APD_{50} are affected by not only Ca^{2+} channels but also other ion channels, such as voltage-gated K^+ channels (I_{to} and I_{Kur}). The present study found that mirabegron reduced I_{Ca-L} but did not alter I_{to} in the RA myocytes. By contrast, mirabegron significantly increased I_{Ca-L} but reduced I_{to} in the LA myocytes. These findings suggested that mirabegron affected the electrophysiological characteristics of the LA and RA differentially, ultimately leading to atrial arrhythmogenesis. The whole-cell patch clamp experiments demonstrated that mirabegron increased I_{Ca-L} and I_{Kur} but reduced I_{to} in the LA myocytes. These results suggested that the shortening of the APD_{20} and APD_{50} of the LA is mainly attributable to the composite effects of mirabegron on I_{Ca-L} , I_{Kur} and I_{to} . The results also indicated that mirabegron did not alter the APD_{90} of the LA and RA. Phase 3 repolarization occurs because of the time-dependent inactivation of I_{Ca-L} and

activation of $I_{K_{r-tail}}$. The $I_{K_{r-tail}}$, rapid component of $I_{K_{r-tail}}$ and slow component of $I_{K_{r-tail}}$ all play major roles in phase 3 repolarization (30). In the current study, $I_{K_{r-tail}}$ in the LA myocytes remained unchanged after mirabegron treatment and this unchanged $I_{K_{r-tail}}$ was responsible for APD₉₀ expression caused by mirabegron in the LA.

The present study had some limitations. First, it found that mirabegron has a direct electrophysiological effect on the LA (an AF substrate), suggesting that mirabegron possibly contributed to atrial arrhythmogenesis. However, simply investigating the acute effects of mirabegron may not reveal the complete mechanisms underlying the arrhythmogenesis induction caused by mirabegron. Chronic mirabegron treatment in patients with overactive bladder may result in the various electrophysiological effects involved in arrhythmogenesis. Second, in the present study, mirabegron increased I_{Ca-L} in the LA myocytes, whereas KT5823 suppressed this effect as well as arrhythmogenesis in the LA. It was also observed that mirabegron significantly increased Ca^{2+}_i and SR Ca^{2+} content, which may result in Ca^{2+} dysregulation. Therefore, mirabegron may induce LA arrhythmogenesis through Ca^{2+} overload induction and activation of cAMP-dependent protein kinase. Although acute mirabegron administration may not alter the expression of RyR, SERCA and PLB due to short experimental periods, it is not clear whether mirabegron may change the phosphorylation of RyR, SERCA and PLB, leading to Ca^{2+} dysregulation in the present study. The precise signaling pathways underlying mirabegron-induced LA arrhythmogenesis were not completely elucidated.

In conclusion, mirabegron differentially modulated the electrophysiological and arrhythmogenic effects in the LA and RA. Through the activation of the cAMP-dependent protein kinase pathway and induction of Ca^{2+} dysregulation, mirabegron may increase LA arrhythmogenesis, increasing AF risk in patients receiving mirabegron treatment.

Acknowledgements

Not applicable.

Funding

This work was supported by the Ministry of Science and Technology of Taiwan (grant no. MOST 110-2314-B-038-126-MY2), Taipei Medical University-Taipei Medical University Hospital (grant no. 108TMU-TMUH-25), Taipei Medical University (grant no. TMU109-AE1-B29) and the Foundation for the Development of Internal Medicine in Okinawa (grant no. 03-009).

Availability of data and materials

The datasets used and/or analyzed during the present study are available from the corresponding authors on reasonable request.

Authors' contributions

CC, YL and CH contributed to analyzing the experimental results and writing the manuscript. FL, CL and YCC contributed to the *in vitro* experiments and provided technical

assistance. SH, SC and YJC contributed to conceiving and designing the study and reviewing the manuscript. CC and YCC confirm the authenticity of all the raw data. All authors read and approved the final manuscript.

Ethics approval and consent to participate

All the experimental procedures were approved by the Institutional Animal Care and Use Committee of Taipei Veterans General Hospital, Taipei, Taiwan (approval no. IACUC-2021-011). Furthermore, the experimental protocols conform to the institutional guideline for the care and use of laboratory animals and the *Guide for the Care and Use of Laboratory Animals* published by the United States National Institutes of Health.

Patient consent for publication

Not applicable.

Competing interests

The authors declare that they have no competing interests.

References

- Gauthier C, Tavernier G, Charpentier F, Langin D and Le Marec H: Functional β_3 -adrenoceptor in the human heart. *J Clin Invest* 98: 556-562, 1996.
- Khullar V, Amarenco G, Angulo JC, Cambroner J, Høye K, Milsom I, Radziszewski P, Rechberger T, Boerrigter P, Drogendijk T, *et al*: Efficacy and tolerability of mirabegron, a β_3 -adrenoceptor agonist, in patients with overactive bladder: Results from a randomised European-Australian phase 3 trial. *Eur Urol* 63: 283-295, 2013.
- Wagg A, Cardozo L, Nitti VW, Castro-Diaz D, Auerbach S, Blauwet MB and Siddiqui E: The efficacy and tolerability of the β_3 -adrenoceptor agonist mirabegron for the treatment of symptoms of overactive bladder in older patients. *Age Ageing* 43: 666-675, 2014.
- Wagg A, Staskin D, Engel E, Herschorn S, Kristy RM and Schermer CR: Efficacy, safety, and tolerability of mirabegron in patients aged ≥ 65 yr with overactive bladder wet: A phase IV, double-blind, randomised, placebo-controlled study (PILLAR). *Eur Urol* 77: 211-220, 2020.
- Gauthier C, Leblais V, Kobzik L, Trochu JN, Khandoudi N, Bril A, Balligand JL and Marec HL: The negative inotropic effect of β_3 -adrenoceptor stimulation is mediated by activation of a nitric oxide synthase pathway in human ventricle. *J Clin Invest* 102: 1377-1384, 1998.
- Moniotte S, Kobzik L, Feron O, Trochu JN, Gauthier C and Balligand JL: Upregulation of β_3 -adrenoceptors and altered contractile response to inotropic amines in human failing myocardium. *Circulation* 103: 1649-1655, 2001.
- Skeberdis VA, Gendvilienė C, Zablockaitė D, Treinys R, Macianskiene R, Bogdelis A, Jurevicius J and Fischmeister R: β_3 -adrenergic receptor activation increases human atrial tissue contractility and stimulates the L-type Ca^{2+} current. *J Clin Invest* 118: 3219-3227, 2008.
- Nitti VW, Khullar V, Kerrebroeck P, Herschorn S, Cambroner J, Angulo JC, Blauwet MB, Dorrepaal C, Siddiqui E and Martin NE: Mirabegron for the treatment of overactive bladder: A prespecified pooled efficacy analysis and pooled safety analysis of three randomised, double-blind, placebo-controlled, phase III studies. *Int J Clin Pract* 67: 619-632, 2013.
- Batista JE, Kölbl H, Herschorn S, Rechberger T, Cambroner J, Halaska M, Coppel A, Kaper M, Huang M and Siddiqui E: The efficacy and safety of mirabegron compared with solifenacin in overactive bladder patients dissatisfied with previous antimuscarinic treatment due to lack of efficacy: results of a noninferiority, randomized, phase IIb trial. *Ther Adv Urol* 7: 167-179, 2015.

10. Nitti VW, Chapple CR, Walters C, Blauwet MB, Herschorn S, Milsom I, Auerbach S and Radziszewski P: Safety and tolerability of the β_3 -adrenoceptor agonist mirabegron, for the treatment of overactive bladder: Results of a prospective pooled analysis of three 12-week randomised phase III trials and of a 1-year randomised phase III trial. *Int J Clin Pract* 68: 972-985, 2014.
11. Lindemann JP, Jones LR, Hathaway DR, Henry BG and Watanabe AM: β -Adrenergic stimulation of phospholamban phosphorylation and Ca^{2+} -ATPase activity in guinea pig ventricles. *J Biol Chem* 258: 464-471, 1983.
12. Takasago T, Imagawa T and Shigekawa M: Phosphorylation of the cardiac ryanodine receptor by cAMP-dependent protein kinase. *J Biochem* 106: 872-877, 1989.
13. Perchenet L, Hinde AK, Patel KC, Hancox JC and Levi AJ: Stimulation of $\text{Na}^+/\text{Ca}^{2+}$ exchange by the β -adrenergic/protein kinase A pathway in guinea-pig ventricular myocytes at 37 degrees C. *Pflugers Arch* 439: 822-828, 2000.
14. Lou Q, Janardhan A and Efimov IR: Remodeling of calcium handling in human heart failure. *Adv Exp Med Biol* 740: 1145-1174, 2012.
15. Heijman J, Voigt N, Wehrens XH and Dobrev D: Calcium dysregulation in atrial fibrillation: the role of CaMKII. *Front Pharmacol* 5: 30, 2014.
16. Pappone C, Rosanio S, Oreto G, Tocchi M, Gugliotta F, Vicedomini G, Salvati A, Dicandia C, Mazzone P, Santinelli V, *et al*: Circumferential radiofrequency ablation of pulmonary vein ostia: A new anatomic approach for curing atrial fibrillation. *Circulation* 102: 2619-2628, 2000.
17. Roithinger FX, Steiner PR, Goseki Y, Sparks PB and Lesh MD: Electrophysiologic effects of selective right versus left atrial linear lesions in a canine model of chronic atrial fibrillation. *J Cardiovasc Electrophysiol* 10: 1564-1574, 1999.
18. Lin YK, Lai MS, Chen YC, Cheng CC, Huang JH, Chen SA, Chen YJ and Lin CI: Hypoxia and reoxygenation modulate the arrhythmogenic activity of the pulmonary vein and atrium. *Clin Sci* 122: 121-132, 2012.
19. Chan CS, Lin YK, Chen YC, Kao YH, Chen SA and Chen YJ: Hydrogen sulphide increases pulmonary veins and atrial arrhythmogenesis with activation of protein kinase C. *J Cell Mol Med* 22: 3503-3513, 2018.
20. Chan CS, Lin YS, Lin YK, Chen YC, Kao YH, Hsu CC, Chen SA and Chen YJ: Atrial arrhythmogenesis in a rabbit model of chronic obstructive pulmonary disease. *Transl Res* 223: 25-39, 2020.
21. National Research Council (US) Committee for the Update of the Guide for the Care and Use of Laboratory Animals: Guide for the care and use of laboratory animals. 8th edition. National Academies Press (US), Washington, DC, 2011.
22. Chan CS, Chen YC, Chang SL, Lin YK, Kao YH, Chen SA and Chen YJ: Heart failure differentially modulates the effects of ivabradine on the electrical activity of the sinoatrial node and pulmonary veins. *J Card Fail* 24: 763-772, 2018.
23. Calvo-Guirado JL, Satorres M, Negri B, Ramirez-Fernandez P, Maté-Sánchez JE, Delgado-Ruiz R, Gomez-Moreno G, Abboud M and Romanos GE: Biomechanical and histological evaluation of four different titanium implant surface modifications: An experimental study in the rabbit tibia. *Clin Oral Invest* 18: 1495-1505, 2014.
24. Chen YJ, Chen YC, Wongcharoen W, Lin CI and Chen SA: Effect of K201, a novel antiarrhythmic drug on calcium handling and arrhythmogenic activity of pulmonary vein cardiomyocytes. *Br J Pharmacol* 153: 915-925, 2008.
25. Lu YY, Chung FB, Chen YC, Tsai CF, Kao YH, Chao TF, Huang JH, Chen SA and Chen YJ: Distinctive electrophysiological characteristics of right ventricular outflow tract cardiomyocytes. *J Cell Mol Med* 18: 1540-1548, 2014.
26. Huang SY, Lu YY, Lin YK, Chen YC, Chen YA, Chung CC, Lin WS, Chen SA and Chen YJ: Ceramide modulates electrophysiological characteristics and oxidative stress of pulmonary vein cardiomyocytes. *Eur J Clin Invest* 52: e13690, 2022.
27. McDonald TF, Pelzer S, Trautwein W and Pelzer DJ: Regulation and modulation of calcium channels in cardiac, skeletal, and smooth muscle cells. *Physiol Rev* 74: 365-507, 1994.
28. Landstrom AP, Dobrev D and Wehrens XHT: Calcium signaling and cardiac arrhythmias. *Circ Res* 120: 1969-1993, 2017.
29. Li D, Zhang L, Kneller J and Nattel S: Potential ionic mechanism for repolarization differences between canine right and left atrium. *Circ Res* 88: 1168-1175, 2001.
30. Grand AO: Cardiac ion channels. *Circ Arrhythm Electrophysiol* 2: 185-194, 2009.



This work is licensed under a Creative Commons Attribution-NonCommercial-NoDerivatives 4.0 International (CC BY-NC-ND 4.0) License.